Published in final edited form as:
Invest Ophthalmol Vis Sci. 2008 October ; 49(10): 4620–4630. doi:10.1167/iovs.08-1816.

Control of Chemokine Gradients by the Retinal Pigment Epithelium

Guangpu Shi, **Arvydas Maminishkis**, **Tina Banzon**, **Stephen Jalickee**, **Rong Li**, **Jeffrey Hammer**, and **Sheldon S. Miller**
From the National Eye Institute, National Institutes of Health, Bethesda, Maryland

Abstract

Purpose—Proinflammatory cytokines in degenerative diseases can lead to the loss of normal physiology and the destruction of surrounding tissues. In the present study, the physiological responses of human fetal retinal pigment epithelia (hfRPE) were examined in vitro after polarized activation of proinflammatory cytokine receptors.

Methods—Primary cultures of hfRPE were stimulated with an inflammatory cytokine mixture (ICM): interleukin (IL)-1β, tumor necrosis factor (TNF)-α, and interferon (IFN)-γ. Western blot analysis and immunofluorescence were used to determine the expression/localization of the cytokine receptors on hfRPE. Polarized secretion of cytokines was measured. A capacitance probe technique was used to measure transepithelial fluid flow (J_V) and resistance (R_T).

Results—IL-1R1 was mainly localized to the apical membrane and TNFR1 to the basal membrane, whereas IFN-γR1 was detected on both membranes. Activation by apical ICM induced a significant secretion of angiogenic and angiostatic chemokines, mainly across the hfRPE apical membrane. Addition of the ICM to the basal but not the apical bath significantly increased net fluid absorption (J_V) across the hfRPE within 20 minutes. Similar increases in J_V were produced by a 24-hour exposure to ICM, which significantly decreased total R_T.

Conclusions—Chemokine gradients across the RPE can be altered (1) through an ICM-induced change in polarized chemokine secretion and (2) through an increase in ICM-induced net fluid absorption. In vivo, both of these factors could contribute to the development of chemokine gradients that help mediate the progression of inflammation/angiogenesis at the retina/RPE/choroid complex.

The retinal pigment epithelium (RPE) is a monolayer of polarized pigmented cells that form the outer blood-retina barrier.[1-3] In the subretinal space (SRS) of the intact eye, the RPE apical membrane is in close physical proximity to the distal ends of the photoreceptors, whereas the basolateral membrane is closely apposed to Bruch's membrane and the choroidal blood supply. The RPE is remarkable in its ability to transport fluid and to secrete a variety of growth and neurotrophic factors and proinflammatory cytokines and chemokines in a polarized manner.[4-9] In vitro, RPE cells have been shown to produce monocyte chemotactic protein (MCP)-1, interleukin (IL)-8, IL-6,[10] regulated on activation of normal T-cell expressed and secreted (RANTES),[11] interferon (IFN)-γ induced protein (IP) of 10 kDa (IP-10),[12] and growth-related oncogene (GRO)-α,[13] with or without stimulation by other proinflammatory cytokines. Together, the secretion of proinflammatory cytokines and chemokines[14-16] and fluid transport[17,18] could act in concert to change the course of inflammatory diseases.

Corresponding author: Sheldon S. Miller, NIH/NEI, 31 Center Drive MSC 2510, Bethesda, MD 20892-2510; millers@nei.nih.gov..
Disclosure: **G. Shi**, None; **A. Maminishkis**, None; **T. Banzon**, None; **S. Jalickee**, None; **R. Li**, None; **J. Hammer**, None; **S.S. Miller**, None

Cytokines are soluble proteinaceous substances (5-20 kDa) produced by a wide variety of cell types that secrete humoral factors and act to modulate the activities of other cells or tissues in normal or pathologic conditions. The functions of cytokines are pleiotropic and redundant. Chemokines are a subfamily of low-molecular-weight cytokines (8-10 kDa) identified by their ability to attract and activate leukocytes. CC and CXC are two structural variants that differ according to variations in a shared cysteine (C) motif. CC chemokines contain adjacent cysteines and are chemoattractants for lymphocytes, monocytes, eosinophils, and basophils, whereas CXC chemokines contain paired cysteines separated by a different amino acid and are chemoattractants for neutrophils. CXC chemokines can be categorized in terms of the "ELR" motif, which has been shown to associate the presence or absence of glutamic acid-leucine-arginine immediately preceding the first cysteine residue of the primary structure of these molecules with proangiogenic activity or its absence with antiangiogenic activity.[19] In addition, some CC chemokines are highly angiogenic.[20,21]

Some chemokines are constitutively expressed in the eye, participate in the normal physiological activities of ocular cells and tissues,[10] and undergo a dramatic increase in expression in diseases such as uveitis,[15,22] diabetic proliferative retinopathy,[23] and age-related macular degeneration (AMD).[24] There is growing evidence that the immunologic properties of the RPE play a critical role in the accumulation of drusen and the progression to choroidal neovascularization (CNV) in AMD.[25-32]

The present study utilizes a previously described hfRPE primary culture model that has the morphology, polarization, and other physiologic properties of intact native tissue.[7] A mixture of three proinflammatory cytokines—IL-1β, IFN-γ, and tumor necrosis factor (TNF)-α—was used to stimulate confluent monolayers of hfRPE. These proinflammatory cytokines have been found to be elevated in animal models of experimental autoimmune uveitis (EAU)[14] and in patients with uveitis.[33,34] Similarly, increased levels of TNF-α and IL-1β are also detected in the vitreous and blood of patients with proliferative diabetic retinopathy (PDR),[35] and in those with AMD with CNV.[36] Our data show that hfRPE expresses the receptors for all three cytokines and that activation of these receptors can dramatically affect the polarized secretion of cytokines/chemokines, alter transepithelial resistance, and increase net epithelial fluid absorption from the retinal to the choroidal side of the monolayer. These experiments suggest how the RPE in vivo can actively control the inflammatory environment in the SRS and choroid.

Methods

Human Fetal Tissue

The research performed in this study adhered to the tenets of the Declaration of Helsinki and the NIH Institutional Review Board. Human fetal eyes of nominal gestation of 15 to 17 weeks were obtained from Advanced Bioscience Resources (Alameda, CA).

Cell Culture

Primary cell cultures of hfRPE cells were prepared from human fetal eyes as described previously.[7] Second-passage cells were seeded in 0.4-μm pore polyester transwells (Transwell; Corning Inc., Corning, NY). Media were changed every 3 days, and the cultures were maintained for 6 weeks before experiments.

Western Blot Analysis and Immunofluorescence

The presence of receptor transcripts for IL-1β, IFN-γ, and TNF-α in hfRPE has been reported previously (Wang F et al. *IOVS* 2006;47:ARVO E-Abstract 2855). The presence of these receptors was confirmed using Western blot analysis and immunofluorescence. For Western

blot analysis, hfRPE cultures were rinsed three times in cold PBS, harvested with a cell scraper, and pelleted at 4°C. The pellet was lysed with RIPA buffer (Sigma-Aldrich, St. Louis, MO) supplemented with complete protease inhibitors for 20 minutes on ice, with periodic vortexing. Cell lysate was centrifuged at 14,000*g* for 10 minutes, and the supernatant was collected. Extracted protein was quantified with a BCA protein assay (Pierce Biotechnology, Rockford, IL). Twenty micrograms of total protein was loaded into each lane of a 4% to 12% gel (NuPAGE; Invitrogen Corp., Carlsbad, CA) under reducing conditions and transferred to nitrocellulose membranes. The membranes were probed with antibodies against IL-1R1 (Abcam, Cambridge, MA), TNFR1, TNFR2 (Stressgen Bioreagents, Ann Arbor, MI), and IFN-γR α chain (Accurate Chemicals, Westbury, NY) and developed with a gel documentation system (Autochemie; UVP, Upland, CA). The cells grown on transwell inserts were stained for cytokeratin and Na,K-ATPase, localized to the apical membrane, to check the purity and polarity.

For immunofluorescence, primary antibodies against ZO-1 (Invitrogen Corp.), Na,K-ATPase (Abcam), IL-1R1, TNFR1, and IFN-γR α chain (R&D Systems, Minneapolis, MN) were labeled with Zenon antibody labeling technology as per the manufacturer's instructions (Invitrogen Corp.). Cultures growing on the membrane inserts were placed on ice and washed three times with cold PBS. The cells were fixed for 30 minutes in 4% formaldehyde, washed three times with PBS, and permeabilized for 30 minutes with 0.2% Triton X-100/PBS. The cells were washed three times with PBS and then blocked with a signal enhancer (Image-IT FX; Invitrogen Corp.) for 30 minutes at room temperature. After being washed three times with PBS, the cells were stained with labeled primary antibody at a 1:100 dilution in PBS, washed three times with PBS, and treated with 4% formaldehyde for an additional 15 minutes at room temperature. The cells were washed three times with PBS, mounted on glass slides with antifade reagent with DAPI (Prolong Gold; Invitrogen Corp.), and imaged (Apotome microscope, Axioplan 2; with Axiovision 3.4 software; Carl Zeiss Meditec, Inc., Dublin, CA).

Stimulation with an Inflammatory Cytokine Mixture

IL-1β (10 ng/mL), TNF-α (10 ng/mL), and IFN-γ (100 IU/mL; PeproTech, Rocky Hill, NJ) were prepared in serum-free medium (SFM) and added separately or as a mixture to the cells growing on transwells and assayed for cytokine/chemokine secretion after 24 hours. The inflammatory cytokine mixture (ICM) or its components in Ringer solution were also used in a modified Üssing chamber for fluid transport measurements. The cytokines were added to either the apical or basal compartments or both. For the cytokine/chemokine secretion assay, culture media were removed and washed with serum-free medium (SFM) containing glutamine-penicillin-streptomycin and nonessential amino-acids, incubated overnight, and then replaced by fresh SFM-containing cytokines.

The transwells are constructed with unequal volumes in the apical and basal baths (0.5 and 1.5 mL, respectively) and therefore it seemed possible that local cytokine activity would be differentially affected. This possibility was tested by adding appropriately constructed O-rings into the basal compartment, which reduced basal side volume in three steps from 1.5 to 0.5 mL. There was no change in liquid level between the apical and basal compartments. The cultures were incubated for 24 hours, and supernatant from both compartments were collected and stored at -80°C for subsequent analysis. Chemokine and cytokine levels were assayed with a commercial technology (SearchLight; Pierce Biotechnology). In this technique, proteome arrays are multiplexed using sandwich ELISAs for the quantitative measurement of 2 to 16 cytokines per sample. This chemiluminescent-based ELISA is typically 2- to 10-fold more sensitive than traditional colorimetric methods and has recently been tested against two other commercial assays.[37] Although these three systems are not in quantitative agreement, the SearchLight assay technology was found to have the highest sensitivity. The variance of this

method was tested by using known amounts of MCP-1 (nominally 20 ng, typically with ±10% variance according to company specs; PeproTech) and IL-8 (nominally 1 ng with ±10% variance; R&D Systems). These cytokines were dissolved in 200 μL of SFM to a final concentration of 100 ± 10 and 1 ± 0.1 ng/mL, respectively, and they compared closely to those obtained from Pierce Biotechnology: 129.2 ± 15 ng/mL for MCP-1 and 1.1 ± 0.1 ng/mL for IL-8 (mean ± SEM; $n = 3$). In control medium (SFM), the mean cytokine levels ($n = 3$) varied from 4×10^{-4} (e.g., IL-6, RANTES, and IL-12p70) to 5×10^{-2} ng/mL (e.g., GRO-α). In each sample, we measured the activities of IL-6 and -12 cytokines as well as CC and CXC subfamily chemokines including MCP-1, macrophage inflammation protein (MIP)-1α, MIP-1β, RANTES, MCP-3, MCP-2, macrophage derived cytokine (MDC), GRO-α, IL-8, monokine induced by IFN-γ (MIG), IP-10, and IFN-inducible T-cell α chemoattractant (I-TAC).

Fluid Transport

Cultured hfRPE monolayers were mounted in a modified Üssing chamber, and rates of transepithelial water flow were measured by using a modified capacitance probe technique, as previously described.[38-40] Tissue physiology, transport potential, and viability were ascertained by concomitantly measuring transepithelial potential (TEP), tissue resistance (R_T), and transepithelial fluid flow (J_V). In these experiments, J_V, TEP, and R_T were recorded for 20 to 30 minutes before addition of the cytokine mixture (ICM in Ringer). ICM was then perfused into one or both bathing solutions on either side of the hfRPE and the recordings continued for another 15 to 60 minutes. In some control experiments, two succeeding cytokines additions were performed to test for reversibility/repeatability of responses. Ringer contained the following (in mM): 100 NaCl, 5 KCl, 23 $NaHCO_3$, 1 $MgCl_2$, 1.8 $CaCl_2$, 0.1 NaH_2PO_4, 0.4 Na_2HPO_4, 2 taurine, 35 sucrose, and 5 glucose. The Ringer was initially bubbled with 5% CO_2-10% O_2-85% N_2, to a pH of ~7.4 and kept inside a CO_2 incubator during the experiment. The osmolarity of the control solution was 295 ± 5 mOsm with no measurable change when the cytokine mixture was added.

Statistics

Unless otherwise noted, all experiments were repeated at least three times and data are presented as the mean ± SEM. Statistical comparisons were made using the Student's *t*-test (unpaired, two tailed, unless otherwise specified; Excel; Microsoft, Redmond, WA). Differences were considered to be significant if $P < 0.05$. The data in Table 1 was log transformed to make the distributions being compared symmetrical.[41]

Results

Expression and Localization of IL-1R, TNF-R, and IFN-γR on hfRPE Plasma Membranes

As a first step in understanding the physiological impact of inflammatory cytokines on hfRPE, we confirmed the presence and location of the corresponding apical and basolateral membrane cognate receptors. IL-1R1, IFN-γR1, and TNFR1, but not TNFR2, expression was confirmed by Western blot in hfRPE. The data in Figure 1 are representative of four primary cultures. IFN-γR1 displayed two bands, close to 100 and 55 kDa, consistent with the observations of Aguet et al.[42] Their analysis indicated that the discrepancy of the molecular weight represented by the two bands is very likely due to different levels of glycosylation. The prominent antibody-specific bands close to 55 and 80 kDa, represent TNFR1[43] and IL-1R1,[44] respectively.

As previously reported,[7] monolayers of hfRPE cells grown on transwells for 6 weeks exhibit the morphology, pigmentation, polarity, and physiology, typical of native RPE.

Figure 2 shows immunofluorescence of the three cytokine receptors located on hfRPE in maximum intensity projections (MIPs). In all three images, each panel shows two *z*-sections

located on the top and right side of each main panel as well as a high gain image of one of the *z*-sections to the right. In all images, DAPI (blue) was used to label the nuclei. ZO-1 is labeled red in Figures 2A and 2B and green in 2C. Figure 2A shows IL-1R1 labeled in green, 2B shows TNFR1 labeled in green, and 2C shows IFN-γR1 labeled in red. The overlap of labels results in additional colors (e.g., in panel A, yellow results from overlap of red and green, corresponding to ZO-1 and IL-1R1). Figure 2A shows that IL-1RI (green signal) is located primarily above the ZO-1 (red) and the DAPI (blue) labeled nuclei, indicating a mainly apical location with some staining on the lateral face of the cell. TNFR1 (green signal) shows a mainly basal localization (Fig. 2B). The basal localization of this receptor is indicated by its appearance below ZO-1 (red signal) and in the same plane as the basally located nuclei (DAPI). The IFN-γR1 signal (red) was detected at most of the basolateral cell membranes and on some apical membranes.

Polarized Secretion of Cytokines/Chemokines by hfRPE

Table 1 summarizes the polarized secretions of simultaneously measured chemokines ($n = 12$) and cytokines ($n = 3$) using multiplex sandwich ELISAs. The left-hand column of this table defines the stimuli and the site of addition of inflammatory mediators. The top two rows of Table 1A show constitutive secretion into the apical or basal bath for unstimulated confluent hfRPE monolayers. Rows 3 to 8 summarize the cytokine secretions to the apical and basal baths after 24 hours' incubation with ICM (IL-1β, TNF-α, and IFN-γ). Each table entry is the mean ± SD of three experiments, with the levels of significance colored coded for ease of comparison (gray; not significant, $P > 0.05$; all other colors indicate different levels of statistical significance from $P < 0.05$ to 0.001). Rows 1 and 2 (apical and basal) summarize two main results: (1) Significant levels of MCP-1, GRO-α, and IL-6 were constitutively secreted into the apical bath; (2) the secretion level of MCP-1 was more than two orders of magnitude greater than that of GRO-α or IL-6.

Rows 3 to 8 (Table 1A) show that addition of ICM to the apical or basal baths produced significant increases in cytokine secretion into both the apical and basal baths for virtually all cytokines tested. Based on the receptor localization data presented in Figure 2, ICM components were added to the apical or basal compartments. A comparison of the middle panels in Tables 1A and 1B shows that ICM components induced far less potent and fewer significant responses (gray bars) than did complete ICM. In Table 1B, a comparison of rows 5 and 6 with rows 1 to 4 shows that concomitant addition of IL-1β to the apical bath and TNF-α and IFN-γ to the basal bath was, in almost all cases, the most effective of the three component stimuli. With only one exception, Table 1B also shows that each component stimuli induced larger changes in the secretion of angiogenic versus angiostatic cytokines/chemokines.[19-21]

Figure 3 summarizes the mean values in Table 1 as a "heat map" for better visualization and comparison of the patterns of ICM-induced chemokine secretion. The heat map variations in color intensity correspond to the measured secretion levels for different combinations of inflammatory mediators added to the apical or basal baths. In Figure 3A, all cytokine levels were measured using apical samples and in Figure 3B, all levels were obtained from basal-side samples. The magnitude of the responses range over 5 log units and therefore all the data were $\log_{10}$ transformed. The lightest shade of yellow corresponds to secretion levels between 0 and 10 pg/mL, and each increment represents a log unit increase in secretion level.

The top row in Figure 3A indicates that only MCP-1 was constitutively secreted in large and significant amounts to the apical bath (≈9 ng/mL; Table 1). Figure 3B, top row, shows that the mean secretion of MCP-1 in to the basal bath noticeably exceeded baseline levels but Table 1 ($n = 3$) shows that this level of secretion did not achieve statistical significance. The subsequent rows in each panel represent the variations in secretion of all the cytokines tested after addition of ICM or its components. In Figures 3A and 3B, the bold vertical lines separate three relatively

distinct clusters of cytokine secretion. The heat map patterns shows that (1) relatively little change in secretion was observed for almost all the non-angiogenesis-regulating cytokines (middle panel); (2) any stimuli added to the apical or basal bath induced more apical than basal secretion (i.e., Fig. 3A secretion levels > Fig. 3B levels); (3) addition of ICM to *apical* or *both* baths produced the largest changes in cytokine secretion into the apical and basal baths; (4) ICM or its components had their largest effects on MCP-1, IL-8, and GRO-α secretion into the apical or basal baths; and (5) the order of secretion magnitude was angiogenic > angiostatic.

The geometry of the transwell dictates that there were unequal bath volumes on each side of the monolayer, to avoid a hydrostatic pressure difference. In the present experiments (Fig. 3, Table 1) hydrostatic pressure was reduced to 0 by maintaining the apical bath volume at 0.5 mL and basal bath volume at 1.5 mL. The activity measurements in Table 1 and Figure 3 are corrected for this volume difference, but there is still the possibility of a potential artifact that cannot be obviated by a simple volume correction. Autocrine pathways may, for example, cause significant differences in activity and subsequent alterations in receptor mediated stimulation at the apical or basolateral membranes. To examine this possibility, cytokine/chemokine secretion into either bath was measured as a function of basal bath volume between 0.5 and 1.5 mL. In the experiments summarized in Figure 4, ICM was added to both bathing solutions. Cytokine secretion into the apical bath (Fig. 4, top) showed no significant variation in activity as a function of basal bath volume change between 0.5 and 1.5 mL (filled, open, and hatched bars; apical bath volume constant). Figure 4, bottom, shows that the reduction of *basal* side volume from 1.5 to 0.5 mL increased the level of detectable cytokines (hatched versus solid bars). This suggests that the volume corrections used in Table 1 and Figure 3 provide the correct basal side activity.

Effects of Inflammatory Cytokines on hfRPE Fluid Transport

Figure 5A shows that addition of ICM to the basal bath increased J_V by ~10 $\mu L \cdot cm^{-2} \cdot h^{-1}$ for the first stimulation and by ~ 3 $\mu L \cdot cm^{-2} \cdot h^{-1}$ for the second stimulation, consistent with an increase in fluid absorption from the retinal to choroidal side of the tissue. Assuming isotonic fluid transport, an increase of 10 $\mu L \cdot cm^{-2} \cdot h^{-1}$ would coincide with an ICM-induced increase in net solute flux of 3 $\mu eq \cdot cm^{-2} \cdot h^{-1}$; or equivalently, 1.5 $\mu eq \cdot cm^{-2} \cdot h^{-1}$ of net Na and Cl flux.[5,6,45] The first J_V response is reversible, with an activation time of 10 to 20 minutes; the second response is diminished, but still reversible. In these experiments, TEP and R_T were used to assess overall transport potential and monolayer integrity, but the chamber design did not allow us to measure relatively fast electrical changes. The apparent changes in TEP and R_T were not seen in two other experiments and are probably artifactual, caused by a solution-induced change in the mechanical seal at the tissue perimeter. In three experiments, mean J_V more than doubled from 6.7 ± 3.1 to 15.5 ± 5.5 $\mu L \cdot cm^{-2} \cdot h^{-1}$ ($P < 0.05$; mean ± SEM, $n = 3$); the mean TEP and R_T in control Ringer were 2.2 ± 0.8 mV and 787 ± 98 $\Omega \cdot cm^2$, respectively ($n = 3$). Figure 5B shows that ICM addition to both bathing solutions increased J_V by ~5 $\mu L \cdot cm^{-2} \cdot h^{-1}$, and there were no significant changes in TEP or R_T ($n = 3$). In three experiments, addition of ICM to both bathing solutions increased mean J_V by ≈50%, from 12.9 ± 5.0 to 18.4 ± 6.4 $\mu L \cdot cm^{-2} \cdot h^{-1}$ ($P < 0.05$). In striking contrast, addition of the ICM to the apical bathing solution did not produce a significant change in J_V, 12.5 ± 0.9 compared with 11.2 ± 0.9 $\mu L \cdot cm^{-2} \cdot h^{-1}$ ($P > 0.1$; $n = 3$).

The ICM-induced changes in J_V could be solely due to the observed polarization of the cytokine receptors. To test this hypothesis, we concomitantly added IL-1β to the apical bathing solution and TNF-α, together with IFN-γ, to the solution bathing the basal side. In Figure 6A, J_V increased by ~13 $\mu L \cdot cm^{-2} \cdot h^{-1}$ and then recovered to baseline after washout of cytokines from both bathing solutions. This experiment showed a small cytokine-induced change in R_T but a significant change was not observed in six cytokine-treated monolayers (365 ± 97 $\Omega \cdot cm^2$ in

control versus 368 ± 94 Ω · cm^2 in treated monolayers). In six experiments, the ICM combination increased mean J_V from 5.4 ± 1.6 to 19 ± 3.6 μL · cm^{-2} · h^{-1} (mean ± SEM; P = 0.005). In control experiments, IL-1β was added to the solution bathing the basal membrane, and concomitantly, TNF-α was added together with IFN-γ to the solution bathing the apical membrane. Figure 6B summarizes the data from a representative experiment with a baseline J_V of ≈15 μL · cm^{-2} · h^{-1}. The cocktail produced no change in J_V and a small change in TEP. In four such experiments, J_V, TEP, and R_T were 12.5 ± 1.1 μL · cm^{-2} · h^{-1}, -0.2± 0.8 mV, 516 ± 70 Ω · cm^2, respectively (mean ± SEM) in the *absence* of this cytokine mixture. In each experiment, subsequent addition of cytokines produced little change. J_V, TEP, and R_T were 11.2 ± 1.1 μL · cm^{-2} · h^{-1}, 0.6± 0.5 mV, 364 ± 80 Ω · cm^2, respectively (P > 0.1). Therefore, mean steady state J_V, TEP, and R_T are unaltered by adding cytokines to the sides of the epithelium apparently lacking their cognate receptors.

The proinflammatory cytokines act acutely to alter J_V (Figs. 5, 6). However, the cytokine secretion experiments summarized in Table 1 and Figure 3 measure a chronic (24 hour) effect of ICM induced cytokine secretion. For a closer comparison of these experiments, we first assessed the constancy of monolayer resistance over 24 hours using the EVOM resistance meter (World Precision Instruments, Sarasota, FL). R_T was measured at t = 0 and t = 24 hours in a total of 10 transwells (five controls and five others to be treated with ICM on *both* sides of the well). These data, summarized in Figure 7, shows that at t = 0, these two groups had no significant difference in mean R_T (328 ± 90 compared with 402 ± 81 Ω · cm^2; n = 5, P = 0.86). The control group resistance at 0 and 24 hours was unchanged (328 ± 90 compared with 381 ± 87 Ω · cm^2; n = 5; P = 0.85). In contrast, addition of ICM for 24 hours to both sides of the cell migration wells significantly decreased R_T from 402 ± 81 Ω · cm^2 to 169 ± 25 Ω · cm^2 (n = 5; P = 0.02). After 24 hours, the ICM-treated wells were significantly decreased in R_T compared with the 24-hour matched control wells (381 ± 87 compared with 169 ± 25 Ω · cm^2 (n = 5; P = 0.04). These matched wells were then transferred to a modified Üssing chamber for measurement of J_V, TEP, and R_T.

The results of the Üssing chamber experiments are summarized in Figure 7 (right) and show that the addition of ICM to both sides of the hfRPE monolayer for 24 hours more than doubled J_V, from 6.0 ± 1.0 to 17.0 ± 2.0 μL · cm^{-2} · h^{-1} (P < 0.002; n = 5). Concomitantly, the mean R_T decreased from 654 ± 143 to 176 ± 34 Ω · cm^2 (P = 0.02; n = 5), whereas the mean TEP (0.3 ± 0.5 mV) was unchanged over this period (P > 0.5).

Therefore, the acute and 24-hour experiments with ICM are comparable in their effects on J_V and TEP, but not in their effects on R_T.

We also added ICM *only* to the apical bath of the hfRPE monolayer for 24 hours. In contrast to the addition of ICM to both sides, apical ICM produced no significant change in J_V (9.0 ± 1.4 μL · cm^{-2} · h^{-1} vs 9.1 ± 2.6 μL · cm^{-2} · h^{-1} (n = 6; P > 0.4), but there was still a significant decrease in mean R_T from 312 to 112 Ω · cm^2 (n = 6; P = 0.004).

Discussion

In the present experiments, we used a model of hfRPE that closely mimics many of the physiological characteristics of adult RPE.[7,46,47] In vivo, the secretion of cytokines/chemokines by the RPE plays a critically important role in the maintenance of an immune specialized environment that is part of the innate immune system and is required for neuronal homeostasis in the retina.[48-52]

Constitutive Secretion of Chemokines by hfRPE: Protective Effects

In the absence of stimuli, hfRPE constitutively secreted physiologically significant quantities of MCP-1 preferentially into the apical bath, and recent evidence from animal models suggests a critical role of this angiogenic chemokine in the development of AMD.[29-31] Other angiogenic chemokines (GRO-α, IL-8, IL-6) were also secreted constitutively by the hfRPE into the SRS, but at much lower levels (Table 1). The latter two chemokines are also part of the downregulatory immune environment of the retina/RPE interface[51] and could participate in the activation of microglia, along with MCP-1.[53,54] As in the CNS,[55] MCP-1 may also protect retinal neurons from glutamate toxicity. The constitutive and induced secretion of this and other chemoattractants (GRO-α, IL-6, or IL-8 in Table 1) to the apical bath may also provide signaling in vivo to attract leukocytes across the RPE to protect the RPE/retina complex (Economopoulou M, et al. *IOVS* 2007;48:ARVO E-Abstract 4925).[29,56] In addition, the secretion and accumulation of MCP-1 in the SRS may require the formation of active dimers or tetramers[57] to provide a mechanism of chronic protection.

ICM-Induced Changes in RPE Secretion of Cytokines/Chemokines: A Model for Damage

Compared with constitutive secretion by the RPE, addition of ICM to the apical bath produced large, physiological changes in the secretion of both angiogenic *and* angiostatic cytokines/chemokines. Analysis of the data summarized in Table 1 and Figure 3 show that, in most cases, the rate of cytokine secretion into the apical bath significantly exceeded that secreted into the basal bath, whether ICM was added to the apical or basal or both baths or IL-1β, TNF-α, or IFN-γ were added, according to the location of their respective cognate receptors (compare Fig. 3A with 3B). Another general conclusion apparent from the data summarized in Figure 3 is that angiogenic cytokines were secreted at a greater rate than were angiostatic cytokines (compare left- and right-hand panels). It is possible that the immunocytochemistry data did not detect small amounts of IL-1R on the basolateral side of the tissue or small amounts of TNFR on the apical side of the tissue. The possible interactions of these receptors and their signaling pathways are currently under study in our laboratory (Li R, et al., manuscript in preparation).

Our observation that stimulated hfRPE cells secrete exceptionally high amounts of MCP-1 onto the apical and basal sides of the cells suggests an important role for this chemokine in diseases that have an inflammatory component, such as CNV.[24] Recently, it has been shown that the MCP-1 released from astrocytes and Müller cells after retinal detachment may be an important determinant of photoreceptor degeneration.[54,58] However, in the absence of a pathophysiologic stimulus, MCP-1 may be protective (see Constitutive Secretion of Chemokines by hfRPE: Protective Effects). There is strong and accumulating evidence that drusen biogenesis and AMD are closely associated with local and chronic inflammation between the RPE basement membrane and Bruch's membrane.[25,59] Dissipation of this protective chemical gradient with age could lead to sub-RPE lipid accumulation, the formation of large drusen, and the progression to CNV.[60]

Polarized secretion of IL-6 and IL-8 was also significantly induced by ICM. IL-8 is a potent chemoattractant for neutrophils and basophils.[61] Both IL-6 and IL-8 are highly angiogenic.[62,63] The preferential secretion of these molecules from the apical side induced by ICM suggests that they play important roles in inflammation and neovascularization in the retina and SRS.[12,50,52,59] We were also surprised to observe that I-TAC and MIG were secreted into the apical bath in substantial amounts (Table 1). These chemokines belong to the CXC family and are generally thought to be angiostatic and involved in the regulation of chemotaxis, cell growth, and T-cell activation.[64] Relatively little is known, however, about the mechanisms by which these particular angiostatic chemokines exert their effects, and their physiological roles in the eye have not been explored. In addition, IP-10, MCP- 3, and RANTES, were also preferably secreted into the apical bath by hfRPE when stimulated by apical ICM. To our

knowledge, the polarized secretion of these angiostatic chemokines has not been previously observed in the eye. We also observed the polarized secretion of GRO-α and MCP-2, both chemoattractants for neutrophils and monocytes, respectively.[65] GRO-α along with other CXCR2 ligands (e.g., IL-8) has been implicated in the pathogenesis of age-related diseases such as Alzheimer's.[66]

Inflammatory Cytokine Stimulates Fluid Absorption across the RPE Monolayer

In vivo, an increase of fluid absorption from the SRS could help regulate the chemical composition of that extracellular space (including cytokines/chemokines). Based on the immunocytochemistry and fluid transport data, acute and after 24 hours (Figs. 2, 5, 6, 7), we can conclude that TNF-α and possibly IFN-γ are the prime determinants of the ICM-induced increase in J_V, whereas IL-1β and IFN-γ may be the prime determinants of the ICM-induced R_T changes. This interpretation of the J_V data is uncertain, because the IFN-γR1 subunit is located on both sides of the cell, whereas IFN-γR2 is located mainly on the basolateral side (data not shown). The detection of IFNR-γR1 on both sides of the cell, and the apical or both-sided ICM-induced changes in R_T, suggest that this subunit is important for controlling transepithelial resistance. We also observed that cytokine secretion induced by apical ICM significantly exceeded that produced by the addition of IL-1 alone into the apical bath (Table 1). TNFR seems clearly localized to the basal side of the cell, which suggests that apical IFNR-γR1 and IL-1R can act synergistically to mediate cytokine secretion. These complex mechanisms are undoubtedly important in understanding the immune system-RPE interaction and required further study.

Fukuda et al.,[17] showed that TNF-α stimulated alveolar fluid clearance, apparently as a result of increased Na uptake by the alveolar epithelial cells. TNF-α was also found to activate 5-nitro 2-(3-phenylpropylamino) benzoate (NPPB)-sensitive Cl channels and Ba-sensitive K channels on rat liver cell line.[67] These two channels are involved in basal Cl and K secretion in human RPE. It is clear that fluid transport across RPE can be driven by Na influx and basal Cl and K secretion.[4-6] IFN-γ was also reported to upregulate the response to UTP, eliciting an intracellular Ca spike and activating Ca-dependent Cl channels in airway epithelial cells.[68] Similar ionic mechanisms may also mediate fluid transport in RPE.[45]

We hypothesize that in inflammatory conditions in vivo, TNF-α or IFN-γ would cause fluid removal from the SRS and therefore increase the activity of any cytokines/chemokines that are present and preferentially secreted by the RPE to the SRS. In addition to the chemokines, molecules such as glutamate, Ca, K, and Na in the SRS could also be concentrated, which would alter photoreceptor function (e.g., dark current) or lead to cell death.[69-71] If the fluid transported from the SRS is allowed to accumulate around Bruch's membrane, this extra volume would cause a *decrease* of chemical activity in the extracellular space just outside the basement membrane. The transfer of volume from the SRS to the choroid per se would increase chemokine gradients across the RPE and drive inflammatory cells toward the SRS.

The acute J_V responses (Figs. 5, 6) seemed puzzling because the ICM-induced changes are thought to be mediated by de novo synthesis of transcription factors and other molecules in the signal transduction pathways of IFN-γ, IL-1β, or TNF-α over a period of hours. These changes in J_V occur in tens of minutes, suggesting that one or more of the ICM components are acting on plasma membrane transporters/receptors or second messengers coupled to active solute-driven fluid transport. Consistent with this finding, several recent studies have shown that lipopolysaccharide (LPS) activation of TLR4 plasma membrane receptors can lead to synthesis NF-$\kappa\beta$ precursors in less than 20 minutes.[72,73]

The secretion data (Table 1, Fig. 3) were obtained after 24 hours of incubation with ICM. This chronic exposure significantly altered the pattern of cytokine/chemokine secretion to the apical/

basal baths, and one would also expect significant changes in hfRPE physiology. This expectation is confirmed by the data summarized in Figure 7, which show that ICM significantly decreased R_T and increased J_V. It is intriguing that both acute and chronic ICM exposure increased J_V, whereas R_T was only affected by chronic exposure. The ICM-induced changes in J_V were due to a direct effect of ICM (acute J_V experiments) with a possible contribution from other cytokines, measured or unmeasured, secreted over the 24-hour period. In vivo, the reduction in R_T would be consistent with the opening of a pathway (paracellular or cellular) that allows immune system cells to reach retinal sites of inflammatory injury.[74-77] In addition, the transmigration of these cells across the RPE from choroid to retina may be significantly enhanced, as indicated earlier, by an increase in chemokine gradients after dehydration of the SRS.

Physiological Implications

The elevation of ICM or its separate components has been observed in a variety of eye diseases —for example, uveitis, PDR, and AMD.[22-24,36,78,79] The initial infiltration of immune cells such as macrophages, neutrophils, or T cells secrete proinflammatory cytokines that trigger an even wider secretory response from the RPE, thus amplifying the inflammatory process. In addition, significant physiologic responses of the RPE may be accompanied by similar responses from other retinal cells, such as microglia.[53]

In PDR, elevated TNF-α and IL-1β were detected in *both* serum (103.8 and 12.8 pg/mL, respectively) and vitreous (160.7 and 34.1 pg/mL, respectively).[35] In addition, elevated MCP-1/CCL2 (2171 pg/mL), IL-8/CXCL8 (173.5 pg/mL),[23,80] and IP-10 (11.7 ng/mL)[23] were measured in the vitreous. The RPE was implicated as a possible source of the accumulated chemokines in the vitreous as might be predicted from the data in Table 1, taking into account dilution effects. Elevated TNF-α and IL-1β in the vitreous or choroidal blood could stimulate RPE from the apical or basolateral sides to secret large amounts of these chemokines. This chemokine accumulation in the retina may account for the aggregation of leukocytes in retinal vessels, causing vessel blockage, and eventual retinal neovascularization.[81]

RPE cells are considered a major source of chemotactic molecules in AMD.[25-27,51,82] We demonstrated in earlier work that these cells constitutively secrete VEGF in a polarized fashion.[7] A possible connection between the proinflammatory stimulus and VEGF was tested in the present studies by measuring the constitutive secretion of VEGF into the apical and basal baths. Constitutive secretion was not significantly altered after 24 hours of ICM stimulation on both sides of the epithelium (data not shown). In AMD the degeneration of RPE cells could alter the uptake of oxidized photoreceptors or affect drusen formation that triggers the release of various cytokines/chemokines, such as IL-8, IL-6, and MCP-1.[82,83] In vivo, the polarized constitutive secretion of MCP-1 and IL-8 into the apical bath would create a chemokine gradient across the RPE that drives monocytes, neutrophils, and T-cells from the choroidal blood vessels toward the RPE basement membrane and then across the RPE monolayer to the SRS. These immune cells would serve to reduce the debris that normally occurs on either side of the RPE after normal metabolic stress and aging.[29-31] The accumulation of immunologically active drusen[25,28] with age can trigger local inflammatory responses that activate immune cells to release further proinflammatory cytokines such as ICM. In addition, the ICM-stimulated release of IL-6 provides a proinflammatory signal that has been shown to promote CNV.[50] Therefore, acute inflammatory alterations in RPE physiology (Figs. 5, 6) are sustained and augmented (Fig. 7), probably by activation of basolateral membrane receptors for TNF-α and IFN-γ, and in vivo may lead to chronic inflammation, CNV, retinal degeneration, and progression to blindness.

Acknowledgments

The authors thank Igal Gery for helpful advice and George Reed for advice on statistics.

Supported by the NEI/NIH Intramural Program.

References

1. Marmor, MF.; Wolfensberger, TJ. The Retinal Pigment Epithelium: Function and Disease. Oxford University Press; New York: 1998.
2. Rizzolo LJ. Development and role of tight junctions in the retinal pigment epithelium. Int Rev Cytol 2007;258:195–234. [PubMed: 17338922]
3. Marmorstein AD. The polarity of the retinal pigment epithelium. Traffic 2001;2:867–872. [PubMed: 11737824]
4. Miller SS, Steinberg RH, Oakley B 2nd. The electrogenic sodium pump of the frog retinal pigment epithelium. J Membr Biol 1978;44:259–279. [PubMed: 313450]
5. Hughes BA, Miller SS, Farber DB. Adenylate cyclase stimulation alters transport in frog retinal pigment epithelium. Am J Physiol 1987;252:C385–C395. [PubMed: 2436482]
6. Edelman JL, Lin H, Miller SS. Acidification stimulates chloride and fluid absorption across frog retinal pigment epithelium. Am J Physiol 1994;266:C946–C956. [PubMed: 8178967]
7. Maminishkis A, Chen S, Jalickee S, et al. Confluent monolayers of cultured human fetal retinal pigment epithelium exhibit morphology and physiology of native tissue. Invest Ophthalmol Vis Sci 2006;47:3612–3624. [PubMed: 16877436]
8. Holtkamp GM, Van Rossem M, de Vos AF, Willekens B, Peek R, Kijlstra A. Polarized secretion of IL-6 and IL-8 by human retinal pigment epithelial cells. Clin Exp Immunol 1998;112:34–43. [PubMed: 9566787]
9. Holtkamp GM, De Vos AF, Peek R, Kijlsta A. Analysis of the secretion pattern of monocyte chemotactic protein-1 (MCP-1) and transforming growth factor-beta 2 (TGF-beta2) by human retinal pigment epithelial cells. Clin Exp Immunol 1999;118:35–40. [PubMed: 10540157]
10. Holtkamp GM, Kijlstra A, Peek R, de Vos AF. Retinal pigment epithelium-immune system interactions: cytokine production and cytokine-induced changes. Prog Retin Eye Res 2001;20:29–48. [PubMed: 11070367]
11. Momma Y, Nagineni CN, Chin MS, Srinivasan K, Detrick B, Hooks JJ. Differential expression of chemokines by human retinal pigment epithelial cells infected with cytomegalovirus. Invest Ophthalmol Vis Sci 2003;44:2026–2033. [PubMed: 12714640]
12. Elner SG, Delmonte D, Bian ZM, Lukacs NW, Elner VM. Differential expression of retinal pigment epithelium (RPE) IP-10 and interleukin-8. Exp Eye Res 2006;83:374–379. [PubMed: 16674942]
13. Crane IJ, Wallace CA, McKillop-Smith S, Forrester JV. Control of chemokine production at the blood-retina barrier. Immunology 2000;101:426–433. [PubMed: 11106948]
14. Foxman EF, Zhang M, Hurst SD, et al. inflammatory mediators in uveitis: differential induction of cytokines and chemokines in Th1-versus Th2-mediated ocular inflammation. J Immunol 2002;168:2483–2492. [PubMed: 11859142]
15. van Kooij B, Rothova A, Rijkers GT, de Groot-Mijnes JD. Distinct cytokine and chemokine profiles in the aqueous of patients with uveitis and cystoid macular edema. Am J Ophthalmol 2006;142:192–194. [PubMed: 16815285]
16. Takase H, Yu CR, Ham DI, et al. inflammatory processes triggered by TCR engagement or by local cytokine expression: differences in profiles of gene expression and infiltrating cell populations. J Leukoc Biol 2006;80:538–545. [PubMed: 16793919]
17. Fukuda N, Jayr C, Lazrak A, et al. Mechanisms of TNF-alpha stimulation of amiloride-sensitive sodium transport across alveolar epithelium. Am J Physiol Lung Cell Mol Physiol 2001;280:L1258–L1265. [PubMed: 11350806]
18. Elia N, Tapponnier M, Matthay MA, et al. Functional identification of the alveolar edema reabsorption activity of murine tumor necrosis factor-alpha. Am J Respir Crit Care Med 2003;168:1043–1050. [PubMed: 12842853]

19. Benelli R, Lorusso G, Albini A, Noonan DM. Cytokines and chemokines as regulators of angiogenesis in health and disease. Curr Pharm Des 2006;12:3101–3115. [PubMed: 16918437]
20. Bernardini G, Ribatti D, Spinetti G, et al. Analysis of the role of chemokines in angiogenesis. J Immunol Methods 2003;273:83–101. [PubMed: 12535800]
21. Hedin KE. Chemokines: new, key players in the pathobiology of pancreatic cancer. Int J Gastrointest Cancer 2002;31:23–29. [PubMed: 12622412]
22. Verma MJ, Lloyd A, Rager H, et al. Chemokines in acute anterior uveitis. Curr Eye Res 1997;16:1202–1208. [PubMed: 9426952]
23. Elner SG, Strieter R, Bian ZM, et al. Interferon-induced protein 10 and interleukin 8. C-X-C chemokines present in proliferative diabetic retinopathy. Arch Ophthalmol 1998;116:1597–1601. [PubMed: 9869787]
24. Grossniklaus HE, Ling JX, Wallace TM, et al. Macrophage and retinal pigment epithelium expression of angiogenic cytokines in choroidal neovascularization. Mol Vis 2002;8:119–126. [PubMed: 11979237]
25. Hageman GS, Luthert PJ, Victor Chong NH, Johnson LV, Anderson DH, Mullins RF. An integrated hypothesis that considers drusen as biomarkers of immune-mediated processes at the RPE-Bruch's membrane interface in aging and age-related macular degeneration. Prog Retin Eye Res 2001;20:705–732. [PubMed: 11587915]
26. Anderson DH, Mullins RF, Hageman GS, Johnson LV. A role for local inflammation in the formation of drusen in the aging eye. Am J Ophthalmol 2002;134:411–431. [PubMed: 12208254]
27. Hageman GS, Hancox LS, Taiber AJ, et al. Extended haplotypes in the complement factor H (CFH) and CFH-related (CFHR) family of genes protect against age-related macular degeneration: characterization, ethnic distribution and evolutionary implications. Ann Med 2006;38:592–604. [PubMed: 17438673]
28. Crabb JW, Miyagi M, Gu X, et al. Drusen proteome analysis: an approach to the etiology of age-related macular degeneration. Proc Natl Acad Sci U S A 2002;99:14682–14687. [PubMed: 12391305]
29. Ambati J, Anand A, Fernandez S, et al. An animal model of age-related macular degeneration in senescent Ccl-2- or Ccr-2-deficient mice. Nat Med 2003;9:1390–1397. [PubMed: 14566334]
30. Tuo J, Bojanowski CM, Zhou M, et al. Murine ccl2/cx3cr1 deficiency results in retinal lesions mimicking human age-related macular degeneration. Invest Ophthalmol Vis Sci 2007;48:3827–3836. [PubMed: 17652758]
31. Combadiere C, Feumi C, Raoul W, et al. CX3CR1-dependent subretinal microglia cell accumulation is associated with cardinal features of age-related macular degeneration. J Clin Invest 2007;117:2920–2928. [PubMed: 17909628]
32. Klein RJ, Zeiss C, Chew EY, et al. Complement factor H polymorphism in age-related macular degeneration. Science 2005;308:385–389. [PubMed: 15761122]
33. Curnow SJ, Falciani F, Durrani OM, et al. Multiplex bead immuno-assay analysis of aqueous humor reveals distinct cytokine profiles in uveitis. Invest Ophthalmol Vis Sci 2005;46:4251–4259. [PubMed: 16249505]
34. Takase H, Futagami Y, Yoshida T, et al. Cytokine profile in aqueous humor and sera of patients with infectious or noninfectious uveitis. Invest Ophthalmol Vis Sci 2006;47:1557–1561. [PubMed: 16565392]
35. Demircan N, Safran BG, Soylu M, Ozcan AA, Sizmaz S. Determination of vitreous interleukin-1 (IL-1) and tumour necrosis factor (TNF) levels in proliferative diabetic retinopathy. Eye 2006;20:1366–1369. [PubMed: 16284605]
36. Cousins SW, Espinosa-Heidmann DG, Csaky KG. Monocyte activation in patients with age-related macular degeneration: a biomarker of risk for choroidal neovascularization? Arch Ophthalmol 2004;122:1013–1018. [PubMed: 15249366]
37. Lash GE, Scaife PJ, Innes BA, et al. Comparison of three multiplex cytokine analysis systems: Luminex, SearchLight and FAST Quant. J Immunol Methods 2006;309:205–208. [PubMed: 16436279]
38. Jiang Y, Grotberg JB. Bolus contaminant dispersion in oscillatory tube flow with conductive walls. J Biomech Eng 1993;115:424–431. [PubMed: 8309238]

39. Maminishkis A, Jalickee S, Blaug SA, et al. The P2Y(2) receptor agonist INS37217 stimulates RPE fluid transport in vitro and retinal reattachment in rat. Invest Ophthalmol Vis Sci 2002;43:3555–3566. [PubMed: 12407168]
40. Edelman JL, Miller SS. Epinephrine stimulates fluid absorption across bovine retinal pigment epithelium. Invest Ophthalmol Vis Sci 1991;32:3033–3040. [PubMed: 1657816]
41. Snedecor, GW.; Cochran, WG. Statistical Methods. 8th ed.. Iowa State University Press; Ames, IA: 1989.
42. Aguet M, Dembic Z, Merlin G. Molecular cloning and expression of the human interferon-gamma receptor. Cell 1988;55:273–280. [PubMed: 2971451]
43. Tartaglia LA, Goeddel DV. Two TNF receptors. Immunol Today 1992;13:151–153. [PubMed: 1322675]
44. Dower SK, Kronheim SR, Hopp TP, et al. The cell surface receptors for interleukin-1 alpha and interleukin-1 beta are identical. Nature 1986;324:266–268. [PubMed: 2946959]
45. Peterson WM, Meggyesy C, Yu K, Miller SS. Extracellular ATP activates calcium signaling, ion, and fluid transport in retinal pigment epithelium. J Neurosci 1997;17:2324–2337. [PubMed: 9065493]
46. Volobueva LA, Killilea DW, Atamna H, Ames BN. N-tert-butyl hydroxylamine, a mitochondrial antioxidant, protects human retinal pigment epithelial cells from iron overload: relevance to macular degeneration. FASEB J 2007;21:4077–4086. [PubMed: 17656467]
47. Li R, Maminishkis A, Wang FE, Miller SS. PDGF-C and -D Induced proliferation/migration of human RPE is abolished by inflammatory cytokines. Invest Ophthalmol Vis Sci 2007;48:5722–5732. [PubMed: 18055825]
48. Canataroglu H, Varinli I, Ozcan AA, Canataroglu A, Doran F, Varinli S. Interleukin (IL)-6, interleukin (IL)-8 levels and cellular composition of the vitreous humor in proliferative diabetic retinopathy, proliferative vitreoretinopathy, and traumatic proliferative vitreoretinopathy. Ocul Immunol inflamm 2005;13:375–381. [PubMed: 16422002]
49. Fahey JV, Schaefer TM, Channon JY, Wira CR. Secretion of cytokines and chemokines by polarized human epithelial cells from the female reproductive tract. Hum Reprod 2005;20:1439–1446. [PubMed: 15734755]
50. Izumi-Nagai K, Nagai N, Ozawa Y, et al. Interleukin-6 receptor-mediated activation of signal transducer and activator of transcription-3 (STAT3) promotes choroidal neovascularization. Am J Pathol 2007;170:2149–2158. [PubMed: 17525280]
51. Nussenblatt RB, Ferris F 3rd. Age-related macular degeneration and the immune response: implications for therapy. Am J Ophthalmol 2007;144:618–626. [PubMed: 17698021]
52. Kanda A, Abecasis G, Swaroop A. Inflammation in the pathogenesis of age-related macular degeneration. Br J Ophthalmol Apr;2008 92(4):448–450. [PubMed: 18369057]
53. Langmann T. Microglia activation in retinal degeneration. J Leukoc Biol 2007;81:1345–1351. [PubMed: 17405851]
54. Nakazawa T, Hisatomi T, Nakazawa C, et al. Monocyte chemoattractant protein 1 mediates retinal detachment-induced photoreceptor apoptosis. Proc Natl Acad Sci U S A 2007;104:2425–2430. [PubMed: 17284607]
55. Eugenin EA, D'Aversa TG, Lopez L, Calderon TM, Berman JW. MCP-1 (CCL2) protects human neurons and astrocytes from NMDA or HIV-tat-induced apoptosis. J Neurochem 2003;85:1299–1311. [PubMed: 12753088]
56. Forrester JV. Macrophages eyed in macular degeneration. Nat Med 2003;9:1350–1351. [PubMed: 14595424]
57. Proudfoot AE, Handel TM, Johnson Z, et al. Glycosaminoglycan binding and oligomerization are essential for the in vivo activity of certain chemokines. Proc Natl Acad Sci U S A 2003;100:1885–1890. [PubMed: 12571364]
58. Nakazawa T, Matsubara A, Noda K, et al. Characterization of cytokine responses to retinal detachment in rats. Mol Vis 2006;12:867–878. [PubMed: 16917487]
59. Gehrs KM, Anderson DH, Johnson LV, Hageman GS. Age-related macular degeneration: emerging pathogenetic and therapeutic concepts. Ann Med 2006;38:450–471. [PubMed: 17101537]

60. Handa JT. New molecular histopathologic insights into the pathogenesis of age-related macular degeneration. Int Ophthalmol Clin 2007;47:15–50. [PubMed: 17237672]
61. Paccaud JP, Schifferli JA, Baggiolini M. NAP-1/IL-8 induces up-regulation of CR1 receptors in human neutrophil leukocytes. Biochem Biophys Res Commun 1990;166:187–192. [PubMed: 2405845]
62. Motro B, Itin A, Sachs L, Keshet E. Pattern of interleukin 6 gene expression in vivo suggests a role for this cytokine in angiogenesis. Proc Natl Acad Sci U S A 1990;87:3092–3096. [PubMed: 1691500]
63. Petzelbauer P, Watson CA, Pfau SE, Pober JS. IL-8 and angiogenesis: evidence that human endothelial cells lack receptors and do not respond to IL-8 in vitro. Cytokine 1995;7:267–272. [PubMed: 7543779]
64. Farber JM. Mig and IP-10: CXC chemokines that target lymphocytes. J Leukoc Biol 1997;61:246–257. [PubMed: 9060447]
65. Charo IF, Ransohoff RM. The many roles of chemokines and chemokine receptors in inflammation. N Engl J Med 2006;354:610–621. [PubMed: 16467548]
66. Xia M, Hyman BT. GROalpha/KC, a chemokine receptor CXCR2 ligand, can be a potent trigger for neuronal ERK1/2 and PI-3 kinase pathways and for tau hyperphosphorylation-a role in Alzheimer's disease? J Neuroimmunol 2002;122:55–64. [PubMed: 11777543]
67. Nietsch HH, Roe MW, Fiekers JF, Moore AL, Lidofsky SD. Activation of potassium and chloride channels by tumor necrosis factor alpha: role in liver cell death. J Biol Chem 2000;275:20556–20561. [PubMed: 10783394]
68. Galietta LJ, Folli C, Caci E, et al. Effect of inflammatory stimuli on airway ion transport. Proc Am Thorac Soc 2004;1:62–65. [PubMed: 16113414]
69. Zeng HY, Zhu XA, Zhang C, Yang LP, Wu LM, Tso MO. Identification of sequential events and factors associated with microglial activation, migration, and cytotoxicity in retinal degeneration in rd mice. Invest Ophthalmol Vis Sci 2005;46:2992–2999. [PubMed: 16043876]
70. Olney JW. The toxic effects of glutamate and related compounds in the retina and the brain. Retina 1982;2:341–359. [PubMed: 6152914]
71. David P, Lusky M, Teichberg VI. Involvement of excitatory neuro-transmitters in the damage produced in chick embryo retinas by anoxia and extracellular high potassium. Exp Eye Res 1988;46:657–662. [PubMed: 2898379]
72. Covert MW, Leung TH, Gaston JE, Baltimore D. Achieving stability of lipopolysaccharide-induced NF-kappaB activation. Science 2005;309:1854–1857. [PubMed: 16166516]
73. Werner SL, Barken D, Hoffmann A. Stimulus specificity of gene expression programs determined by temporal control of IKK activity. Science 2005;309:1857–1861. [PubMed: 16166517]
74. Stamatovic SM, Keep RF, Kunkel SL, Andjelkovic AV. Potential role of MCP-1 in endothelial cell tight junction 'opening': signaling via Rho and Rho kinase. J Cell Sci 2003;116:4615–4628. [PubMed: 14576355]
75. Xu H, Manivannan A, Dawson R, et al. Differentiation to the CCR2+ inflammatory phenotype in vivo is a constitutive, time-limited property of blood monocytes and is independent of local inflammatory mediators. J Immunol 2005;175:915–6923.
76. Muller WA. Leukocyte-endothelial-cell interactions in leukocyte transmigration and the inflammatory response. Trends Immunol 2003;24:327–334. [PubMed: 12810109]
77. Zen K, Parkos CA. Leukocyte-epithelial interactions. Curr Opin Cell Biol 2003;15:557–564. [PubMed: 14519390]
78. Elner SG, Elner VM, Jaffe GJ, Stuart A, Kunkel SL, Strieter RM. Cytokines in proliferative diabetic retinopathy and proliferative vitreoretinopathy. Curr Eye Res 1995;14:1045–1053. [PubMed: 8585935]
79. Yuuki T, Kanda T, Kimura Y, et al. inflammatory cytokines in vitreous fluid and serum of patients with diabetic vitreoretinopathy. J Diabetes Complications 2001;15:257–259. [PubMed: 11522500]
80. Hernandez C, Segura RM, Fonollosa A, Carrasco E, Francisco G, Simo R. Interleukin-8, monocyte chemoattractant protein-1 and IL-10 in the vitreous fluid of patients with proliferative diabetic retinopathy. Diabet Med 2005;22:719–722. [PubMed: 15910622]

81. Miyamoto K, Khosrof S, Bursell SE, et al. Prevention of leukostasis and vascular leakage in streptozotocin-induced diabetic retinopathy via intercellular adhesion molecule-1 inhibition. Proc Natl Acad Sci U S A 1999;96:10836–10841. [PubMed: 10485912]

82. Kijlstra A, La Heij E, Hendrikse F. Immunological factors in the pathogenesis and treatment of age-related macular degeneration. Ocul Immunol Inflamm 2005;13:3–11. [PubMed: 15804763]

83. Higgins GT, Wang JH, Dockery P, Cleary PE, Redmond HP. Induction of angiogenic cytokine expression in cultured RPE by ingestion of oxidized photoreceptor outer segments. Invest Ophthalmol Vis Sci 2003;44:1775–1782. [PubMed: 12657621]

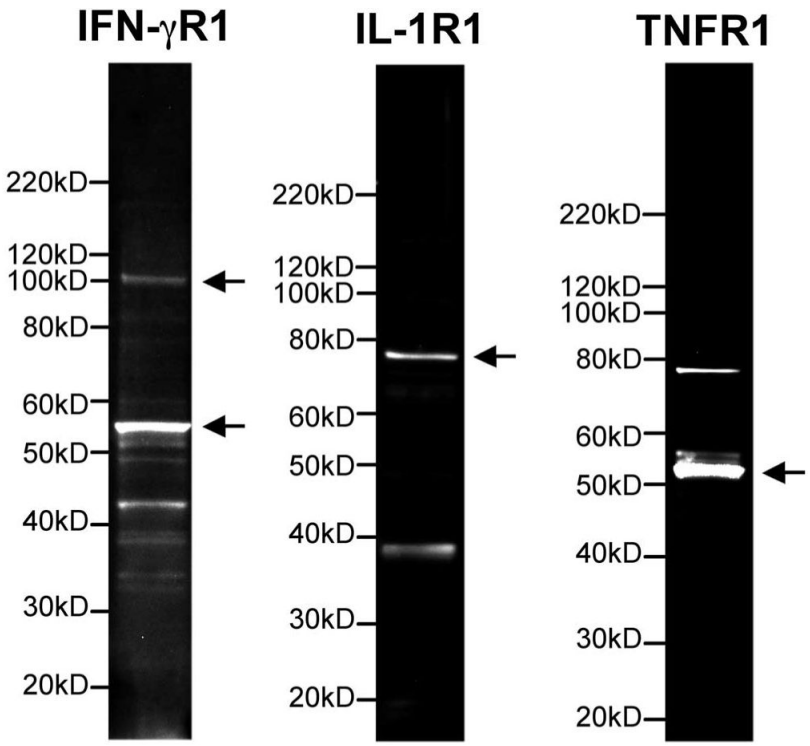

Figure 1.
Western blot analysis to identify IFN-γR1, IL-1R1, and TNFR1. IFN-γR1 displayed two bands, close to 100 and 55 kDa. TNFR1, and IFN-γR1 were detected at approximately 55 and 80 kDa, respectively.

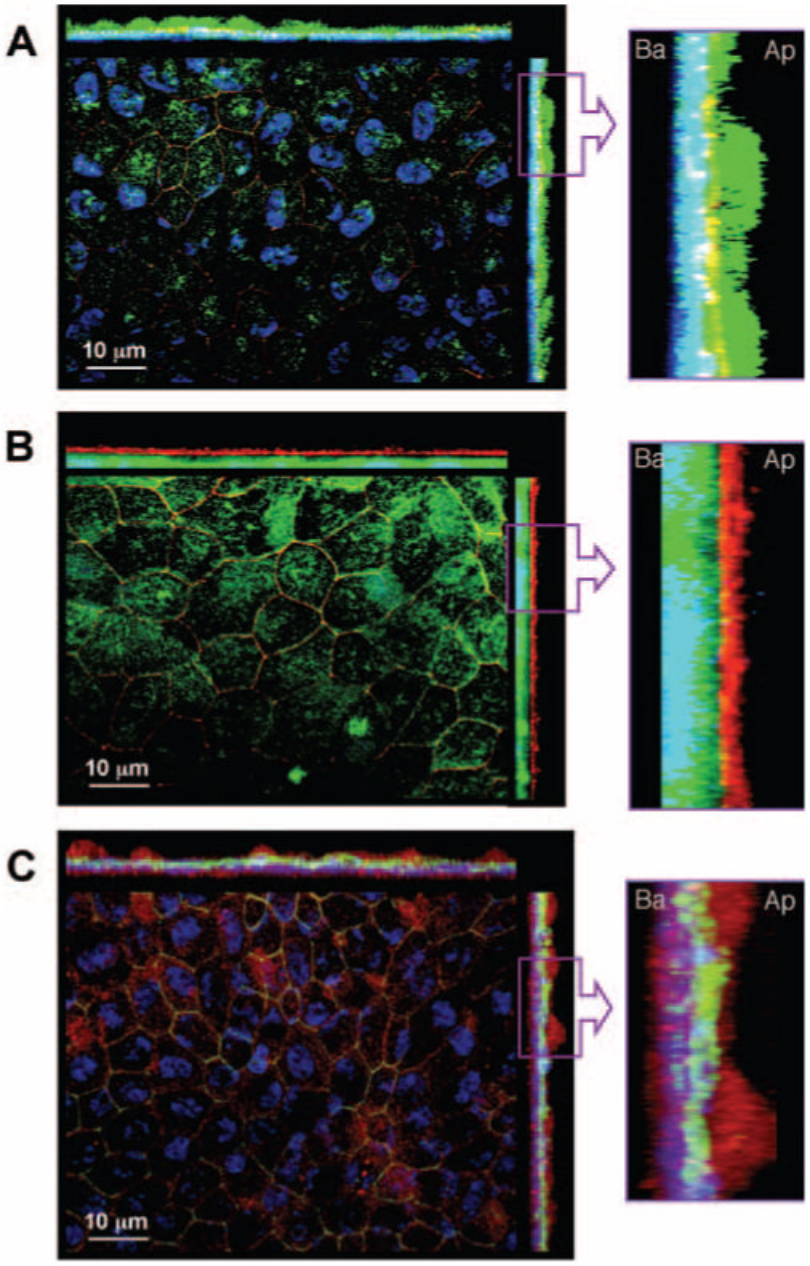

Figure 2.

Immunofluorescence staining of hfRPE cultures grown on transwells. In each part of the figure, the *left* panel is an en face view of the apical membrane shown as a set of superimposed sections (MIP image). For each of the three en face views, the *x*- and *y*-axis side views are also shown as MIP images. In each case, the *right* panel shows a part of the *y*-axis side view image (labeled area) at higher magnification. ZO-1 highlights cell circumferences in the en face images. In the side view, ZO-1 also marks the boundary between the apical and basolateral membranes. (**A**) IL-1R1 (*green*) was mainly localized apically (ZO-1, *yellow*). (**B**) TNF-R1 (*green*) was mainly localized to the basal side (basal ZO-1, *red*). (**C**) IFN-γR1 (*red*) was localized to both the apical and basolateral membranes (ZO-1, *green*). In all three panels, nuclei of the cells were stained with DAPI (*blue*).

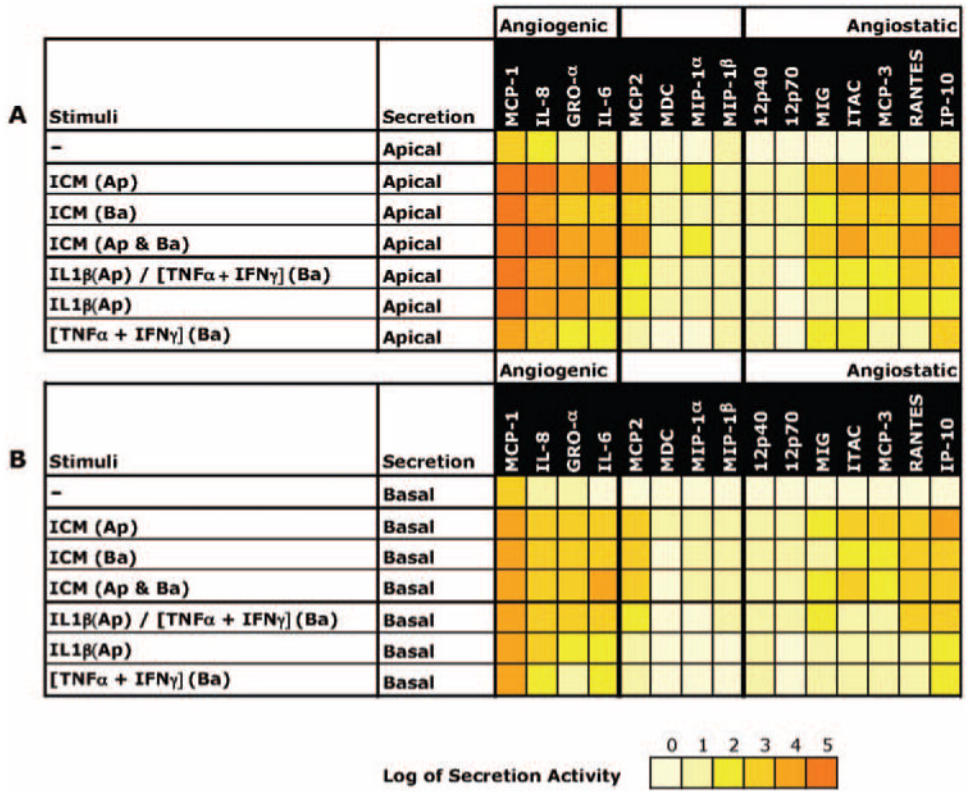

Figure 3.

Summary of mean chemokine secretion levels as a heat map. The heat map variations in color intensity correspond to the measured secretion levels for different combinations of inflammatory mediators added to the apical or basal baths. The data were $\log_{10}$ transformed; the lightest shade of *yellow* corresponds to secretion levels between 0 and 10 pg/mL and each increment represents a log unit increase in secretion level.

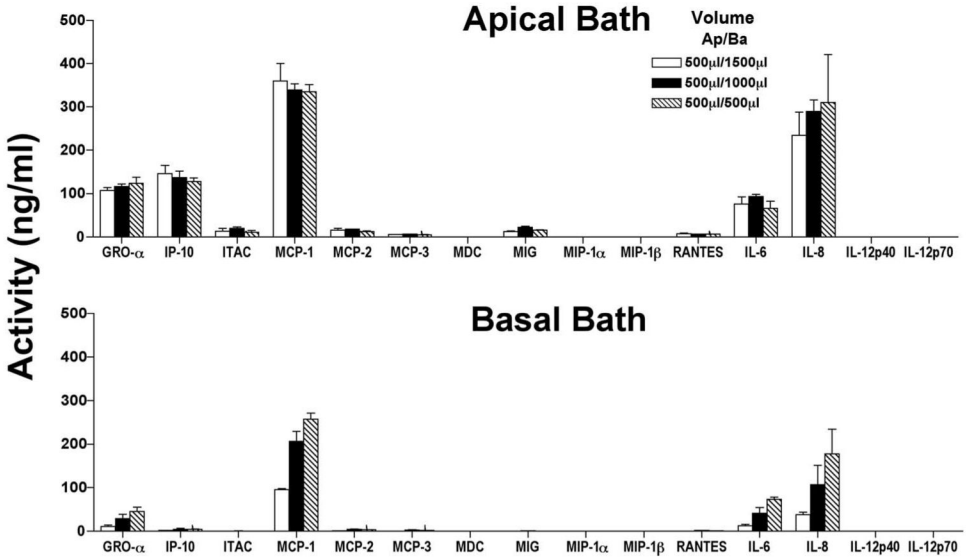

Figure 4.

hfRPE monolayers were stimulated by addition of ICM to both the apical and basal baths for 24 hours (n = 3). Cytokine and chemokine activities were measured in the apical (*top*) and basal (*bottom*) baths after the reduction of basal bath volume in three steps from 1500 to 500 μL. The basal volumes were adjusted with O-rings.

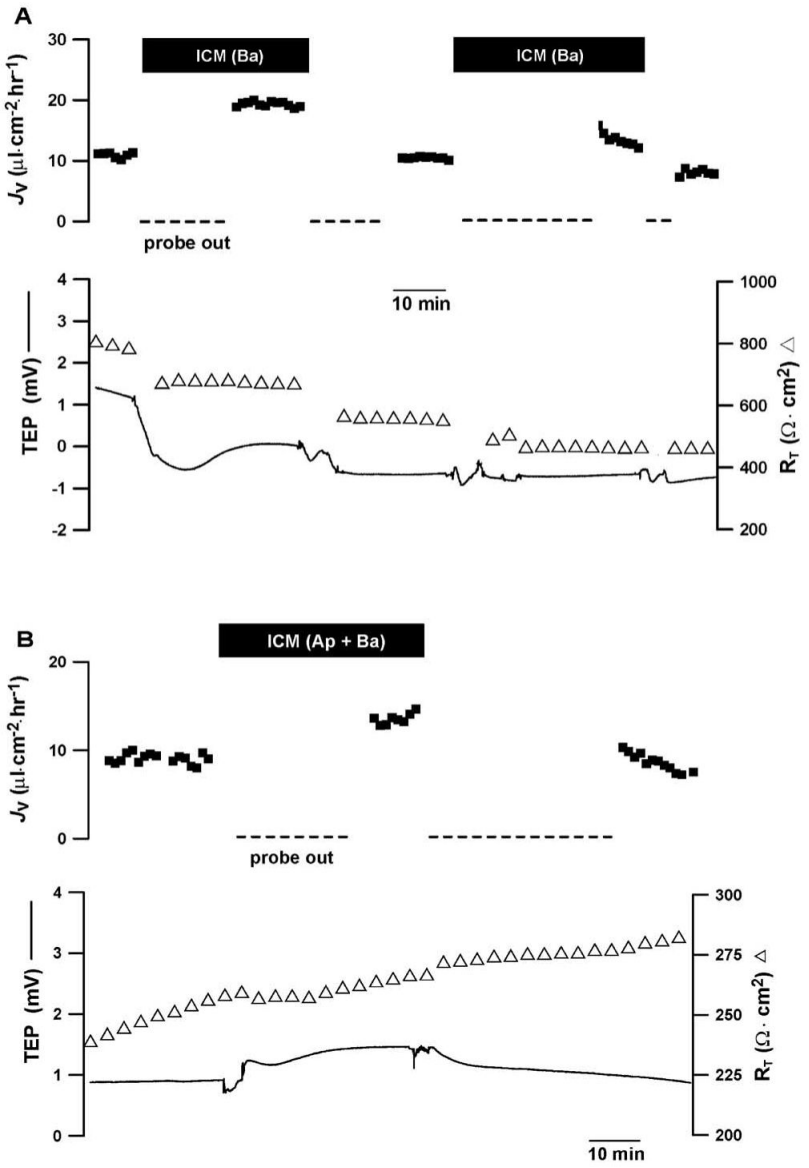

Figure 5.

ICM induced changes in hfRPE fluid transport. *Top traces:* J_V plotted as a function of time, with net fluid absorption is indicated by positive values; *bottom traces*: TEP and R_T are plotted as function of time. (**A**) Addition of ICM to the basal bath increased J_V ~10 μL · cm^{-2} · h^{-1} with no significant changes in TEP and R_T. (**B**) Concomitant addition of ICM to apical and basal baths increased J_V ~5 μL · cm^{-2} · h^{-1} with no changes in TEP and a slight increase in resistance that was not consistent from experiment to experiment. In four experiments, the mean change in R_T was not statistically significant. We used the Student's *t*-test to analyze these acute responses to ICM (paired, two tailed).

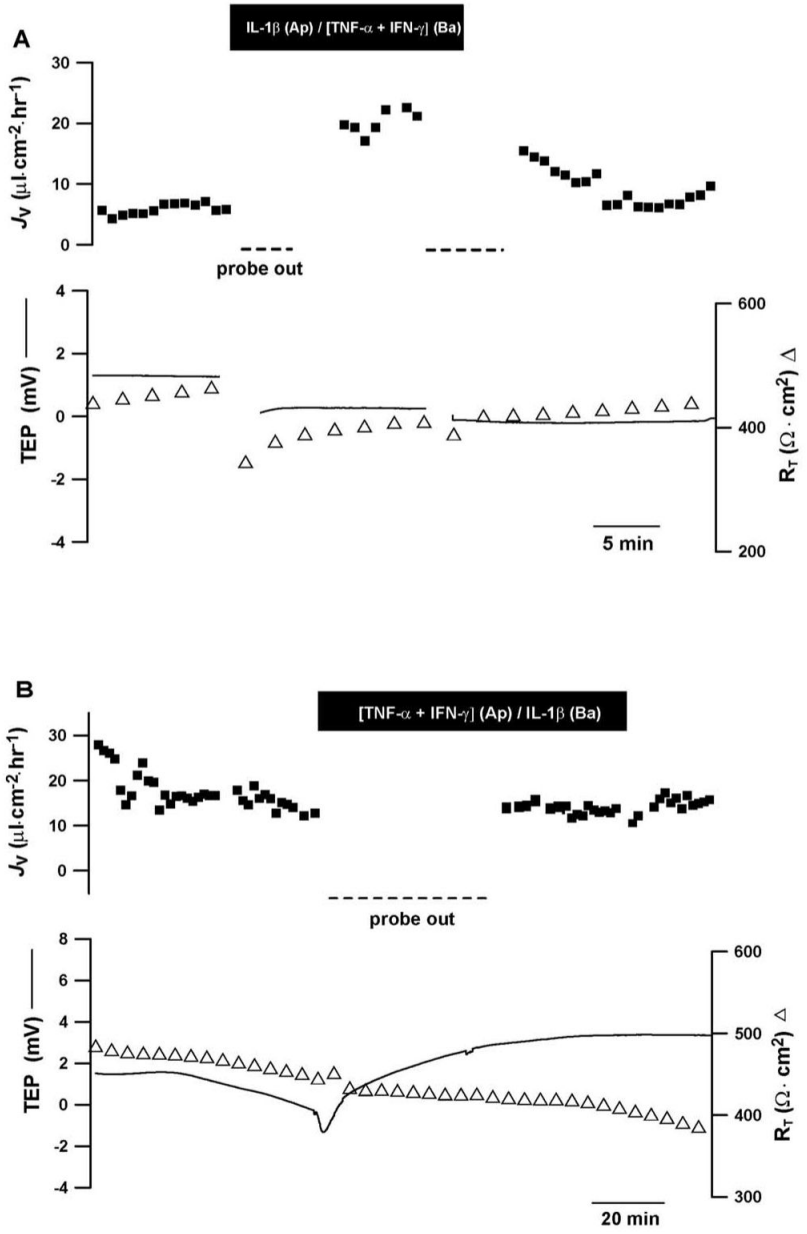

Figure 6.

ICM-induced changes in hfRPE fluid transport, formatted as in Figure 5. (**A**) Addition of IL-1β to the apical and IFN-γ+TNF-α to the basal baths consistent with their primary receptor locations increased J_V ~13 μL · cm^{-2} · h^{-1}. (**B**) Addition of these component cytokines to the bath opposite their primary receptor location did not appreciably alter J_V, R_T, or TEP (n = 4). Student's t-test used to analyze acute responses to ICM components (paired, two-tailed).

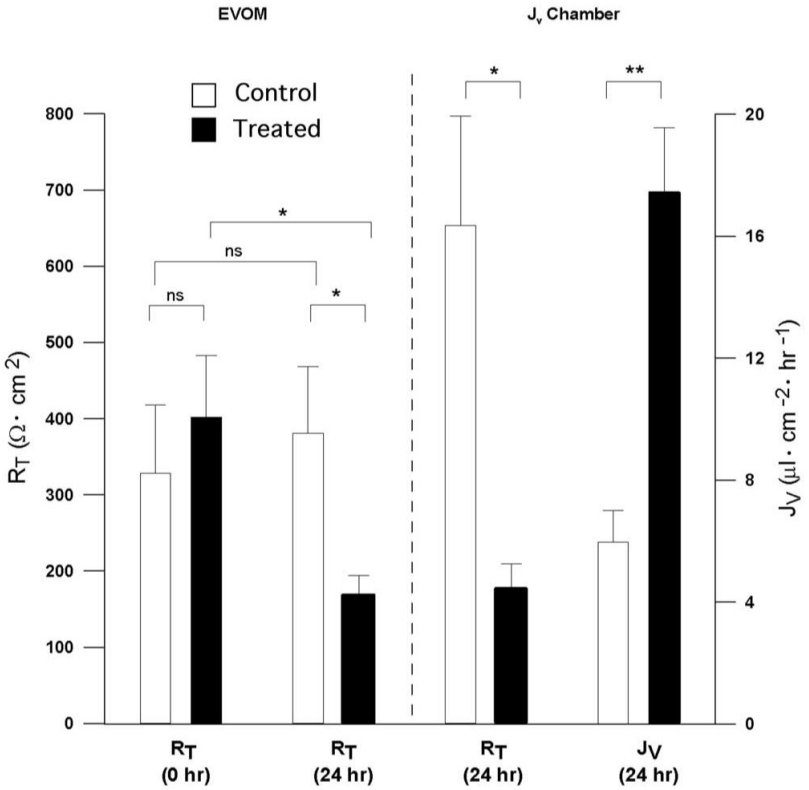

Figure 7.

Twenty-four-hour ICM-induced changes in hfRPE fluid transport and R_T. R_T and J_V summary for hfRPE monolayers treated with ICM in both apical and basal bath for 24 hours and hfRPE control monolayers. R_T decrease was statistically significant for ICM-treated filters at $t = 0$ versus $t = 24$ hours (*$P < 0.05$). A statistically significant increase in J_V was observed in control versus 24-hour ICM-treated filters (**$P < 0.01$). NS, nonsignificant.

Table 1

Effect of ICM on Polarized Secretion of Chemokines and Cytokines by hfRPE

A

		Angiogenic								Angiostatic						
		MCP-1	IL-8	GRO-α	IL-6	MCP-2	MDC	MIP-1α	MIP-1β	12p40	12p70	MIG	ITAC	MCP-3	RANTES	IP-10
Stimuli	Secretion	pg/ml	pg/ml	pg/ml	pg/ml	pg/ml	pg/ml	pg/ml	pg/ml	pg/ml	pg/ml	pg/ml	pg/ml	pg/ml	pg/ml	pg/ml
None	Apical	9,495	647	70.2	55.1	9.6	3.0	7.9	18.6	9.7	1.1	8.8	8.2	14.4	0.6	11.1
	SD	5,285	979	45.9	28.2	6.9	1.4	3.1	17.0	12.9	0.5	6.0	8.6	5.8	0.8	4.0
	Basal	992	95.2	24.4	3.5	3.6	1.4	6.2	9.2	3.7	0.6	3.4	3.7	4.0	0.4	5.0
	SD	1,343	238	29.7	3.1	2.0	1.5	3.6	9.3	7.8	0.3	5.4	2.2	3.3	0.0	4.1
ICM (Ap)	Apical	212,408	110,865	72,097	125,167	34,185	21.9	143	39.5	63.3	40.1	8,518	89,126	22,431	21,067	239,839
	SD	52,434	33,309	1,518	6,565	2,575	2.8	115	13.6	7.2	13.5	3,550	3,409	2,381	2,237	37,493
	Basal	75,019	4,415	2,328	3,221	2,900	10.8	36.8	26.2	51.3	19.9	132	1,335	1,452	4,915	11,700
	SD	8,694	213	191	330	501	0.5	8.7	5.6	4.7	3.8	28.8	250	428	707	1,291
ICM (Ba)	Apical	179,247	22,567	8,375	7,108	6,613	12.9	44.2	24.2	66.2	36.3	202	3,623	1,741	1,088	17,626
	SD	36,462	11,316	2,710	1,457	1,844	1.7	7.5	3.6	6.5	5.8	61.6	1,390	431	244	5,605
	Basal	48,470	2,053	1,227	1,550	1,527	9.0	31.9	21.1	42.4	26.0	94.6	838	622	2,497	5,549
	SD	16,646	309	297	281	492	1.2	1.8	3.8	6.9	5.6	13.1	34.4	263	635	1,661
ICM (Ap & Ba)	Apical	314,290	112,416	39,406	52,479	21,120	11.7	249	81.8	29.2	58.6	6,668	66,863	8,415	9,277	132,548
	SD	99,378	20,528	19,909	26,200	8,537	7.6	104.9	30.3	27.2	55.9	3,754	22,992	4,342	6,159	62,068
	Basal	73,521	4,599	3,363	17,929	2,900	5.0	69.9	51.3	15.1	16.9	138	1,395	623	1,984	7,546
	SD	15,277	2,402	2,039	24,194	1,469	1.9	16.1	15.1	21.5	6.0	37.9	714	252	2,004	4,079

B

		Angiogenic								Angiostatic						
		MCP-1	IL-8	GRO-α	IL-6	MCP-2	MDC	MIP-1α	MIP-1β	12p40	12p70	MIG	ITAC	MCP-3	RANTES	IP-10
		pg/ml	pg/ml	pg/ml	pg/ml	pg/ml	pg/ml	pg/ml	pg/ml	pg/ml	pg/ml	pg/ml	pg/ml	pg/ml	pg/ml	pg/ml
IL1β(Ap)	Apical	107,865	51,298	31,578	7,572	373	14.5	22.4	30.2	50.7	9.5	74.6	27.4	706	580	236
	SD	18,455	14,956	12,362	3,219	309	3.1	7.4	7.2	8.7	1.5	25.3	8.2	470	419	111
	Basal	19,902	1,420	805	318	13.4	4.4	5.8	7.0	23.8	2.6	50.9	30.1	17.5	25.4	184
	SD	9,520	971	634	15.7	3.2	0.5	2.5	2.1	10.3	0.4	53.6	32.4	2.0	16.8	270
[TNFα, IFNγ](Ba)	Apical	73,113	2,358	514	729	14.0	6.5	3.1	10.2	29.7	4.3	153	184	30.3	40.8	3,155
	SD	1,294	1,422	504	30.1	5.0	1.5	0.0	2.1	8.7	1.3	57.0	49.9	7.7	20.2	472
	Basal	28,098	437	98.8	283	11.1	4.1	3.1	5.3	16.1	2.5	161	64.5	15.3	72.8	678
	SD	6,962	98.1	3.9	33.3	1.5	0.2	0.0	0.5	2.8	0.2	72.9	2.6	1.5	31.2	167
IL1β(Ap)/[TNFα, IFNγ](Ba)	Apical	169,963	66,722	42,890	9,935	586	16.5	18.4	28.6	42.1	8.9	282	453	584	1,005	5,524
	SD	35,717	2,751	27,066	4,532	170	4.4	6.4	11.6	5.5	2.4	33.1	544	479	638	1,954
	Basal	59,938	7,959	4,134	2,636	310	6.8	6.3	13.9	42.9	10.3	174	88.6	72.9	207	1,283
	SD	8,945	2,286	904	498	25.2	1.5	2.8	4.7	10.4	6.2	1.4	38.4	7.1	67.9	273

P< 0.05 0.01 0.001 P>0.05

Summary of the polarized secretions of simultaneously measured chemokines (n = 12) and cytokines (n = 3) using multiplex sandwich ELISAs. **A**. Secretion into media with addition of ICM; **B**. Secretion into media with addition of individual components. The left-hand column defines the stimuli and the site of addition of proinflammatory mediators. These data are reported as actual concentrations and therefore are corrected for volume differences on the apical and basal sides of the membrane insert (Transwell; Corning). Each entry is the mean ± SD of three experiments, and the levels of significance are color coded for ease of comparison.